

# Relativistic Hydrodynamics at RHIC and LHC

Tetsufumi HIRANO<sup>1,\*</sup>)

<sup>1</sup> *Department of Physics, The University of Tokyo, Tokyo 113-0033, Japan*

Recent development of a hydrodynamic model is discussed by putting an emphasis on realistic treatment of the early and late stages in relativistic heavy ion collisions. The model, which incorporates a hydrodynamic description of the quark-gluon plasma with a kinetic approach of hadron cascades, is applied to analysis of elliptic flow data at the Relativistic Heavy Ion Collider energy. It is predicted that the elliptic flow parameter based on the hybrid model increases with the collision energy up to the Large Hadron Collider energy.

## §1. Introduction

One of the important discoveries made at the Relativistic Heavy Ion Collider (RHIC) in Brookhaven National Laboratory is that the elliptic flow parameter,<sup>1)</sup> namely, the second Fourier coefficient  $v_2 = \langle \cos(2\phi) \rangle$  of the azimuthal momentum distribution  $dN/d\phi$ ,<sup>2)</sup> is quite large in non-central Au+Au collisions.<sup>3)</sup> Over the past years, many studies have been devoted to understanding the elliptic flow from dynamical models: (1) The observed  $v_2$  values near midrapidity at low transverse momentum ( $p_T$ ) in central and semi-central collisions are consistent with predictions from ideal hydrodynamics.<sup>4)</sup> (2) The  $v_2$  data cannot be interpreted by hadronic cascade models.<sup>5),6)</sup> (3) A partonic cascade model<sup>7)</sup> can reproduce these data only with significantly larger cross sections than the ones obtained from the perturbative calculation of quantum chromodynamics. The produced dynamical system is beyond the description of naive kinetic theories. Thus, a paradigm of the strongly coupled/interacting/correlated matter is being established in the physics of relativistic heavy ion collisions.<sup>8)</sup> The agreement between hydrodynamic predictions and the data suggests that the heavy ion collision experiment indeed provides excellent opportunities for studying matter in local equilibrium at high temperature and for drawing information of the bulk and transport properties of the quark-gluon plasma (QGP). These kinds of phenomenological studies closely connected with experimental results, so to say, the “observational QGP physics”, will be one of the main trends in modern nuclear physics in the eras of the RHIC and the upcoming Large Hadron Collider (LHC). Then it is indispensable to sophisticate hydrodynamic modeling of heavy ion collisions for making quantitative statements on properties of the produced matter with estimation of uncertainties. In fact, the ideal fluid dynamical description gradually breaks down as one studies peripheral collisions<sup>4)</sup> or moves away from midrapidity.<sup>9),10)</sup> This requires a more realistic treatment of the early and late stages<sup>11)–14)</sup> in dynamical modeling of relativistic heavy ion collisions.

In this paper, recent studies of the state-of-the-art hydrodynamic simulations are highlighted with emphases on the importance of the final decoupling stage (Sec. 3)

---

\*) e-mail address: hirano@phys.s.u-tokyo.ac.jp

and of much better understanding of initial conditions (Sec. 4). A prediction of the  $v_2$  parameter at the LHC energy will be made in Sec. 5. See also other reviews<sup>15)</sup> to complement other topics of hydrodynamics in heavy ion collisions at RHIC.

## §2. A QGP fluid + hadronic cascade model

We have formulated a dynamical and unified model,<sup>13)</sup> based on fully three-dimensional (3D) ideal hydrodynamics,<sup>9),10)</sup> toward understanding the bulk and transport properties of the QGP. During the fluid dynamical evolution one assumes local thermal equilibrium. However, this assumption can be expected to hold only during the intermediate stage of the collision. In order to extract properties of the QGP from experimental data one must therefore supplement the hydrodynamic description by appropriate models for the beginning and end of the collision. In Sec. 3, we employ the Glauber model for initial conditions in hydrodynamic simulations. Initial entropy density is parametrized as a superposition of terms scaling with the densities of participant nucleons and binary collisions, suitably generalized to account for the longitudinal structure of the initial fireball.<sup>13)</sup> Instead, in Secs. 4 and 5, we employ the Color Glass Condensate (CGC) picture<sup>17)</sup> for colliding nuclei and calculate the produced gluon distributions<sup>18)</sup> as input for the initial conditions in the hydrodynamical calculation.<sup>19)</sup> During the late stage, local thermal equilibrium is no longer maintained due to expansion and dilution of the matter. We treat this gradual transition from a locally thermalized system to free-streaming hadrons via a dilute interacting hadronic gas by employing a hadronic cascade model<sup>20)</sup> below a switching temperature of  $T^{\text{sw}} = 169$  MeV. A massless ideal parton gas equation of state (EOS) is employed in the QGP phase ( $T > T_c = 170$  MeV) while a hadronic resonance gas model is used at  $T < T_c$ . When we use the hydrodynamic code all the way to final decoupling, we take into account<sup>10)</sup> chemical freezeout of the hadron abundances at  $T^{\text{ch}} = 170$  MeV, separated from thermal freezeout of the momentum spectra at a lower decoupling temperature  $T^{\text{th}}$ , as required to reproduce the experimentally measured yields.<sup>21)</sup>

## §3. Success of a hybrid approach

Initial conditions in 3D hydrodynamic simulations are put so that centrality and pseudorapidity dependences of charged particle yields are reproduced. A linear combination of terms scaling with the number of participants and that of binary collisions enables us to describe centrality dependence of particle yields at midrapidity. This agreement with the data still holds when the ideal fluid description is replaced by a more realistic hadronic cascade below  $T^{\text{sw}}$ . See also Fig. 3. When ideal hydrodynamics is utilized all the way to kinetic freezeout,  $T^{\text{th}} = 100$  MeV is needed to generate enough radial flow for reproduction of proton  $p_T$  spectrum at midrapidity. One major advantage of the hybrid model over the ideal hydrodynamics is that the hybrid model automatically describes freezeout processes without any free parameters. The hybrid model works remarkably well in reproduction of  $p_T$  spectra for identified hadrons below  $p_T \sim 1.5$  GeV/ $c$ .

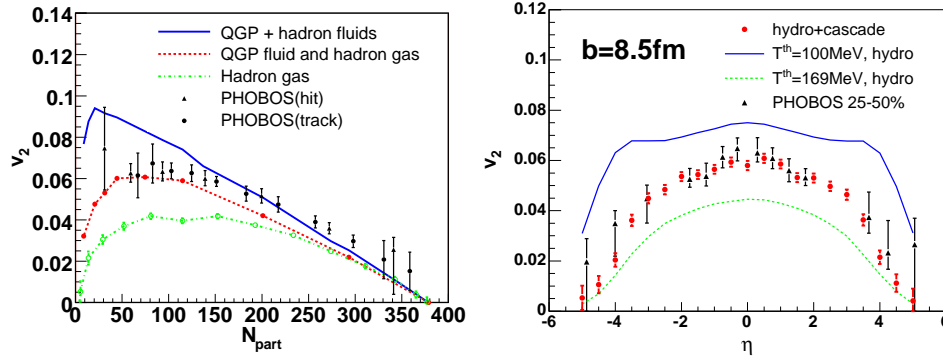


Fig. 1. (Left) Centrality dependence of  $v_2$ . The solid (dashed) line results from a full ideal fluid dynamic approach (a hybrid model). For reference, a result from a hadronic cascade model<sup>6)</sup> is also shown (dash-dotted line). (Right) Pseudorapidity dependence of  $v_2$ . The solid (dashed) line is the result from a full ideal hydrodynamic approach with  $T^{\text{th}} = 100$  MeV ( $T^{\text{th}} = 169$  MeV). Filled circles are the result from the hybrid model. All data are from the PHOBOS Collaboration.<sup>22)</sup>

The centrality dependences of  $v_2$  at midrapidity ( $|\eta| < 1$ ) from (1) a hadronic cascade model<sup>6)</sup> (dash-dotted), (2) a QGP fluid with hadronic rescatterings taken through a hadronic cascade model (dashed), and (3) a QGP+hadron fluid with  $T^{\text{th}} = 100$  MeV (solid) are compared with the PHOBOS data.<sup>22)</sup> A hadronic cascade model cannot generate enough elliptic flow to reproduce the data. This is observed also in other hadronic cascade calculations.<sup>5)</sup> Thus it is almost impossible to interpret the  $v_2$  data from a hadronic picture only. Models based on a QGP fluid generate large elliptic flow and gives  $v_2$  values which are comparable with the data. When a hadronic matter is also treated by ideal hydrodynamics,  $v_2$  is overpredicted in peripheral collisions. This is improved by dissipative effects in the hadronic matter. Note that there could exist effects of eccentricity fluctuation,<sup>23)</sup> which is not taken into account in the current approach. Deviation between the data and the QGP-fluid-based results above  $N_{\text{part}} \sim 200$  could be attributed to these effects.

From the integrated elliptic flow data at midrapidity, initial push from QGP pressure turns out to be important at midrapidity. In Fig. 1 (right), the pseudorapidity dependence of  $v_2$  data in 25-50% centrality observed by PHOBOS<sup>22)</sup> are compared with QGP fluid models. Ideal hydrodynamics with  $T^{\text{th}} = 169$  MeV, which is just below the transition temperature  $T_c = 170$  MeV, underpredicts the data in the whole pseudorapidity region. Hadronic rescatterings after QGP fluid evolution generate the right amount of elliptic flow and, consequently, the triangle pattern of the data is reproduced well. If the hadronic matter is also assumed to be described by ideal hydrodynamics until  $T^{\text{th}} = 100$  MeV,  $v_2$  overshoots in forward/backward rapidity regions ( $|\eta| \sim 4$ ). This is simply due to the fact that, in ideal hydrodynamics,  $v_2$  is approximately proportional to the initial eccentricity which is almost independent of space-time rapidity. So the hadronic dissipation is quite important in forward/backward rapidity regions as well as at midrapidity in peripheral collisions ( $N_{\text{part}} < 100$ ). From these studies, the perfect fluidity of the QGP is needed to

obtain enough amount of the integrated  $v_2$ , while the dissipation (or finite values of the mean free path among hadrons) in the hadronic matter is also important to obtain less elliptic flow coefficients when the multiplicity is small at midrapidity in peripheral collisions and/or in forward/backward rapidity regions. This is exactly the novel picture of dynamics in relativistic heavy ion collisions, namely, the nearly perfect fluid QGP core and the highly dissipative hadronic corona, addressed in Ref. 16)

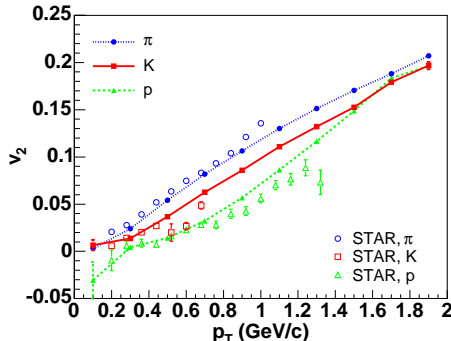


Fig. 2. Transverse momentum dependence of  $v_2$  for pions, kaons and protons. Filled plots are the results from the hybrid model. The impact parameter in the model simulation is 7.2 fm which corresponds to 20-30% centrality. Data (open plots) for pions, kaons and protons are obtained by the STAR Collaboration.<sup>24)</sup>

As a cross-check on the picture, we also study  $p_T$  dependence of  $v_2$  for identified hadrons in semi-central collisions to see whether the hybrid model works. We correctly reproduce mass ordering behavior of differential elliptic flow below  $p_T \sim 1$  GeV/ $c$  as shown in Fig. 2. Here experimental data are from STAR.<sup>24)</sup> Although we also reproduce the data in 10-20% and 30-40% well (not shown), it is hard to reproduce data in very central collisions (0-5%) due to a lack of initial eccentricity fluctuation in this model. It is worth mentioning that, recently, the hybrid model succeeds to describes differential elliptic flow data for identified hadrons at forward rapidity observed by BRAHMS.<sup>25)</sup>

#### §4. Challenge for a hydrodynamic approach

So far, an ideal hydrodynamic description of the QGP fluid with the Glauber type initial conditions followed by an kinetic description of the hadron gas describes the space-time evolution of bulk matter remarkably well. The CGC,<sup>17)</sup> whose cases are growing both in deep inelastic scatterings and in  $d$ +Au collisions recently, is one of the relevant pictures to describe initial colliding nuclei in high energy collisions. In this section, novel hydrodynamic initial conditions<sup>19)</sup> based on the CGC are employed for an analysis of elliptic flow.

We first calculate the centrality dependence of the multiplicity to see that the CGC indeed correctly describes the initial entropy production and gives proper initial conditions for the fluid dynamical calculations. Both CGC and Glauber model initial

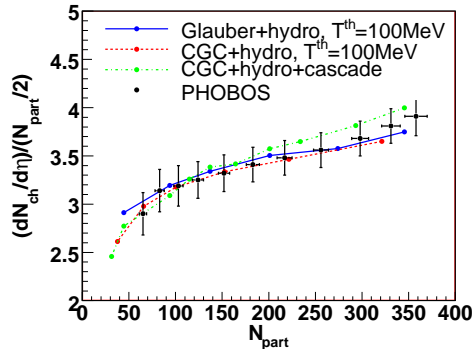


Fig. 3. Centrality dependence of charged particle multiplicity per number of participant nucleons. The solid (dashed) line results from Glauber-type (CGC) initial conditions. The dash-dotted line results from our hybrid model. Experimental data are from PHOBOS.<sup>27)</sup>

conditions, propagated with ideal fluid dynamics, reproduce the observed centrality dependence of the multiplicity,<sup>27)</sup> see Fig. 3. In the hydrodynamic simulations, the numbers of stable hadrons below  $T^{\text{ch}}$  are designed to be fixed by introducing chemical potential for each hadron.<sup>10)</sup> On the other hand, the number of charged hadrons is approximately conserved during hadronic cascades. So the centrality dependence of charged particle yields is also reasonably reproduced by the hybrid approach.

In the left panel of Fig. 4 we show the impact parameter dependence of the eccentricity of the initial energy density distributions at  $\tau_0 = 0.6 \text{ fm}/c$ . We neglect event-by-event eccentricity fluctuations although these might be important for very central and peripheral events.<sup>23)</sup> Even though both models correctly describe the centrality dependence of the multiplicity as shown in Fig. 3, they exhibit a significant difference: The eccentricity from the CGC is 20-30% larger than that from the Glauber model.<sup>13), 28)</sup> The situation does not change even when we employ the “universal” saturation scale<sup>29)</sup> in calculation of gluon production. The initial eccentricity is thus quite sensitive to model assumptions about the initial energy deposition which can be discriminated by the observation of elliptic flow. The centrality dependence of  $v_2$  from the CGC initial conditions followed by the QGP fluid plus the hadron gas is shown in Fig. 4 (right). With Glauber model initial conditions,<sup>4)</sup> the predicted  $v_2$  from ideal fluid dynamics overshoots the peripheral collision data.<sup>22)</sup> Hadronic dissipative effects within hadron cascade model reduce  $v_2$  and, in the Glauber model case, are seen to be sufficient to explain the data (Fig. 1 (left)).<sup>13)</sup> Initial conditions based on the CGC model, however, lead to larger elliptic flows which overshoot the data even after hadronic dissipation is accounted for,<sup>13)</sup> unless one additionally assumes significant shear viscosity also during the early QGP stage. Therefore precise understanding of the bulk and transport properties of QGP from the elliptic flow data requires a better understanding of the initial stages in heavy ion collisions.

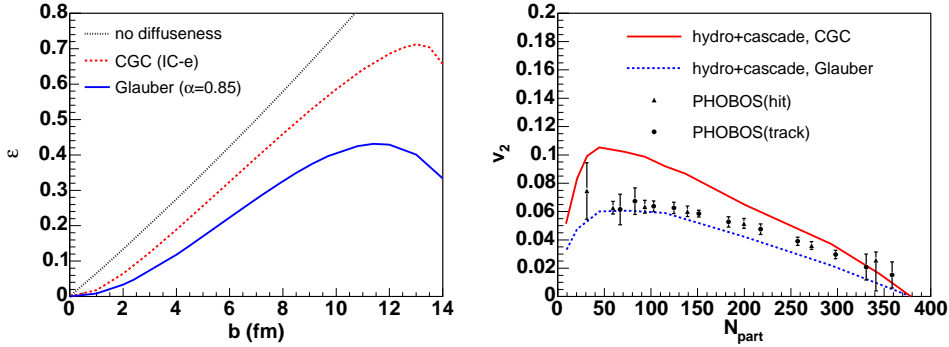


Fig. 4. (Left) Impact parameter dependence of the eccentricity of the initial energy density distributions. The solid (dashed) line results from Glauber-type (CGC) initial conditions. The dotted line assumes a box profile for the initial energy density distribution. (Right) Centrality dependence of  $v_2$ . The solid (dashed) line results from CGC (Glauber model) initial conditions followed by ideal fluid QGP dynamics and a dissipative hadronic cascade. The data are from PHOBOS.<sup>22)</sup>

## §5. Elliptic flow at LHC

The elliptic flow parameter plays a very important role in understanding global aspects of dynamics in heavy ion collisions at RHIC. It must be also important to measure elliptic flow parameter at the LHC energy toward comprehensive understanding of the degree and mechanism of thermalization and the bulk and transport properties of the QGP.

Figure 5 shows the excitation function of the charged particle elliptic flow  $v_2$ , scaled by the initial eccentricity  $\varepsilon$ , for Au+Au collisions at  $b = 6.3$  fm impact parameter, using three different models: (i) a pure 3D ideal fluid approach with a typical kinetic freezeout temperature  $T^{\text{th}} = 100$  MeV where both QGP and hadron gas are treated as ideal fluids (dash-dotted line); (ii) 3D ideal fluid evolution for the QGP, with kinetic freezeout at  $T^{\text{th}} = 169$  MeV and no hadronic rescattering (dashed line); and (iii) 3D ideal fluid QGP evolution followed by hadronic rescattering below  $T^{\text{sw}} = 169$  MeV (solid line). Although applicability of the CGC model for SPS energies might be questioned, we use it here as a systematic tool for obtaining the energy dependence of the hydrodynamic initial conditions. By dividing out the initial eccentricity  $\varepsilon$ , we obtain an excitation function for the scaled elliptic flow  $v_2/\varepsilon$  whose shape should be insensitive to the facts that CGC initial conditions produce larger eccentricities and the resulting integrated  $v_2$  overshoots the data at RHIC and also that experiments with different collision system (Pb+Pb) will be performed at the LHC. Figure 5 shows the well-known bump in  $v_2/\varepsilon$  at SPS energies ( $\sqrt{s_{NN}} \sim 10$  GeV) predicted by the purely hydrodynamic approach, as a consequence of the softening of the equation of state (EOS) near the quark-hadron phase transition region,<sup>30)</sup> and that this structure is completely washed out by hadronic dissipation,<sup>12)</sup> consistent with the experimental data.<sup>31),32)</sup> Even at RHIC energies, hadronic dissipation still reduces  $v_2$  by  $\sim 20\%$ . The hybrid model predicts a monotonically increasing excita-

tion function for  $v_2/\varepsilon$  which keeps growing from RHIC to LHC energies,<sup>12)</sup> contrary to the ideal fluid approach whose excitation function almost saturates above RHIC energies.<sup>30)</sup>

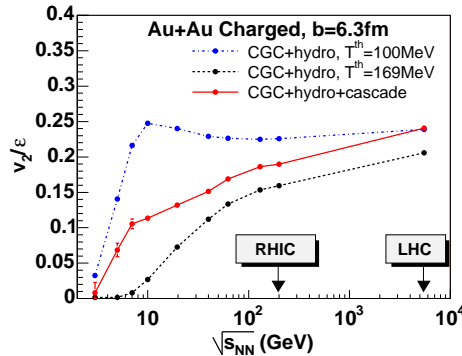


Fig. 5. Excitation function of  $v_2/\varepsilon$  in Au+Au collisions at  $b = 6.3$  fm. The solid line results from CGC initial conditions followed an ideal QGP fluid and a dissipative hadronic cascade. The dashed (dash-dotted) line results from purely ideal fluid dynamics with thermal freezeout at  $T^{\text{th}} = 169$  MeV (100 MeV).

## §6. Conclusions

We have studied the recent elliptic flow data at RHIC by using a hybrid model in which an ideal hydrodynamic treatment of the QGP is combined with a hadronic cascade model. With the Glauber-type initial conditions, the space-time evolution of the bulk matter created at RHIC is well described by the hybrid model. The agreement between the model results and the data includes  $v_2(N_{\text{part}})$ ,  $v_2(\eta)$ ,  $p_T$  spectra for identified hadron below  $p_T \sim 1.5$  GeV/ $c$  and  $v_2(p_T)$  for identified hadrons at midrapidity and in the forward rapidity region. If the Glauber type initial conditions are realized, we can establish a picture of the nearly perfect fluid of the QGP core and the highly dissipative hadronic corona. However, in the case of the CGC initial conditions, the energy density profile in the transverse plane is more “eccentric” than that from the conventional Glauber model. This in turn generates large elliptic flow, which is not consistent with the experimental data. Without viscous effects even in the QGP phase, we cannot interpret the integrated elliptic flow at RHIC. If one wants to extract informations on the properties of the QGP, a better understanding of the initial stages is required. We have also calculated an excitation function of elliptic flow scaled by the initial eccentricity and found that the function continuously increases with collision energy up to the LHC energy when hadronic dissipation is taken into account.

## Acknowledgments

The author would like to thank M. Gyulassy, U. Heinz, D. Kharzeev, R. Lacey and Y. Nara for collaboration and fruitful discussions. He is also much indebted to

T. Hatsuda and T. Matsui for continuous encouragement to the present work. He also thanks M. Isse for providing him with a result from a hadronic cascade model shown in Fig. 1. This work was partially supported by JSPS grant No.18-10104.

### References

- 1) J. Y. Ollitrault, Phys. Rev. D **46** (1992), 229
- 2) A. M. Poskanzer and S. A. Voloshin, Phys. Rev. C **58** (1998), 1671
- 3) B.B. Back *et al.* [PHOBOS Collaboration], Nucl. Phys. A **757** (2005), 28; J. Adams *et al.* [STAR Collaboration], Nucl. Phys. A **757** (2005), 102; K. Adcox *et al.* [PHENIX Collaboration], Nucl. Phys. A **757** (2005), 184
- 4) P. F. Kolb, P. Huovinen, U. W. Heinz and H. Heiselberg, Phys. Lett. B **500** (2001), 232; P. Huovinen *et al.*, Phys. Lett. B **503** (2001), 58
- 5) M. Bleicher and H. Stöcker, Phys. Lett. B **526** (2002), 309; E. L. Bratkovskaya, W. Cassing and H. Stöcker, Phys. Rev. C **67** (2003), 054905; W. Cassing, K. Gallmeister and C. Greiner, Nucl. Phys. A **735** (2004), 277
- 6) P. K. Sahu *et al.*, Pramana **67** (2006), 257; M. Isse, private communication
- 7) D. Molnar and M. Gyulassy, Nucl. Phys. A **697** (2002), 495 [Erratum Nucl. Phys. A **703** (2002), 893]
- 8) T.D. Lee, Nucl. Phys. A **750** (2005), 1; M. Gyulassy and L. McLerran, Nucl. Phys. A **750** (2005), 30; E. Shuryak, Nucl. Phys. A **750** (2005), 64
- 9) T. Hirano, Phys. Rev. C **65** (2001), 011901
- 10) T. Hirano and K. Tsuda, Phys. Rev. C **66** (2002), 054905
- 11) A. Dumitru *et al.*, Phys. Lett. B **460** (1999), 411; S.A. Bass *et al.*, Phys. Rev. C **60** (1999), 021902; S.A. Bass and A. Dumitru, Phys. Rev. C **61** (2000), 064909
- 12) D. Teaney, J. Lauret and E. V. Shuryak, Phys. Rev. Lett. **86** (2001), 4783; nucl-th/0110037; D. Teaney, Phys. Rev. C **68** (2003), 034913
- 13) T. Hirano *et al.*, Phys. Lett. B **636** (2006), 299
- 14) C. Nonaka and S. A. Bass, Phys. Rev. C **75** (2007), 014902
- 15) P. F. Kolb and U. W. Heinz, in *Quark Gluon Plasma 3*, edited by R.C. Hwa and X.N. Wang (World Scientific, Singapore, 2004), p634, nucl-th/0305084; T. Hirano, Acta Phys. Polon. B **36** (2005), 187; Y. Hama, T. Kodama and O. Socolowski Jr., Braz. J. Phys. **35** (2005), 24; F. Grassi, Braz. J. Phys. **35** (2005), 52; P. Huovinen and P. V. Ruuskanen, nucl-th/0605008; C. Nonaka, nucl-th/0702082
- 16) T. Hirano and M. Gyulassy, Nucl. Phys. A **769** (2006), 71
- 17) E. Iancu and R. Venugopalan, in *Quark Gluon Plasma 3*, edited by R.C. Hwa and X.N. Wang (World Scientific, Singapore, 2004), p249, hep-ph/0303204
- 18) D. Kharzeev and M. Nardi, Phys. Lett. B **507** (2001), 121; D. Kharzeev and E. Levin, Phys. Lett. B **523** (2001), 79; D. Kharzeev, E. Levin and M. Nardi, Phys. Rev. C **71** (2005), 054903; D. Kharzeev, E. Levin and M. Nardi, Nucl. Phys. A **730** (2004), 448
- 19) T. Hirano and Y. Nara, Nucl. Phys. A **743** (2004), 305
- 20) Y. Nara *et al.*, Phys. Rev. C **61** (2000), 024901
- 21) P. Braun-Munzinger, D. Magestro, K. Redlich and J. Stachel, Phys. Lett. B **518** (2001), 41
- 22) B. B. Back *et al.* [PHOBOS Collaboration], Phys. Rev. C **72** (2005), 051901
- 23) M. Miller and R. Snellings, nucl-ex/0312008; X.I. Zhu, M. Bleicher and B. Stoecker, Phys. Rev. C **72** (2005), 064911; R. Andrade *et al.*, Phys. Rev. Lett. **97** (2006), 202302; H.J. Drescher and Y. Nara, Phys. Rev. C **75** (2007), 034905
- 24) J. Adams *et al.* [STAR Collaboration], Phys. Rev. C **72** (2005), 014904
- 25) S. J. Sanders, nucl-ex/0701076; nucl-ex/0701078
- 26) B. B. Back *et al.* [PHOBOS Collaboration], Phys. Rev. C **65** (2002), 061901
- 27) B.B. Back *et al.* [PHOBOS Collaboration], Phys. Rev. C **65** (2002), 061901
- 28) A. Kuhlman, U. W. Heinz and Y. V. Kovchegov, Phys. Lett. B **638** (2006), 171; A. Adil *et al.*, Phys. Rev. C **74** (2006), 044905
- 29) T. Lappi and R. Venugopalan, Phys. Rev. C **74** (2006) 054905
- 30) P.F. Kolb, J. Sollfrank and U. Heinz Phys. Rev. C **62** (2000), 054909
- 31) C. Alt *et al.* [NA49 Collaboration], Phys. Rev. C **68** (2003), 034903
- 32) C. Adler *et al.* [STAR Collaboration], Phys. Rev. C **66** (2002), 034904